

Submitted to the

International Symposium on Snow Monitoring and Avalanches (ISSM-2004)
Manali, India

Variations in the mechanical properties of arctic and subarctic snow at local (1-m) to regional (100-km) scales

Matthew Sturm, Jerry Johnson, and Jon Holmgren
U.S. Army Cold Regions Research and Engineering Laboratory-Alaska
P.O. Box 35170
Ft. Wainwright, AK 99703
msturm@crrel.usace.army.mil

Abstract

The mechanical properties of the snow pack were measured at 10 stations in northwest Alaska. Spanning 325 km, the stratigraphy at these stations revealed a ubiquitous hard wind slab overlying multiple layers of depth hoar. At each station five closely spaced (0.2 m) resistance profiles were recorded using a micropenetrometer. Using a micro-mechanical theory, we have converted the high-frequency residual saw-tooth response of the micropenetrometer into grain size, pore size, and bond strength as a function of depth. A comparison of the resistance strength of slab layers within and between stations indicates that local variations were as large as regional variations. This variability is attributed to wind eddies and drifting snow producing mini-dunes with stoss (hard) and lee (soft) slopes. Measurements taken from a subarctic snow pack intersecting a thick melt crust showed a similarly high local variance. We conclude that high local variance is likely in most types of snow packs. The implications of these findings with respect to avalanches are that a) large ranges in layer strength and properties are to be expected over short distances, particularly in mountain settings, and b) it may be possible to measure the full local range of properties across relatively short (10-m) transects.

Introduction

When a weak layer of snow fails, it can trigger an avalanche. As a consequence, there has been considerable research into the characteristics of weak layers (Gubler, 1977; McClung and Schaerer, 1993; Davis and others, 1996; 1998; Fierz, 1998; Colbeck and Jamieson, 2001), and speculation about how extensive they must be to function as triggers (Smith and Sommerfeld, 1985; Gubler and Bader, 1989; Conway and Abrahamson, 1984). Rutschblock, stuffblock, and other stability tests (Föhn, 1987; Jamieson and Johnston, 1993; Birkeland and others, 1996) tacitly assume that a layer which is weak over an area of just a few square meters will also be weak over an area large enough to trigger an avalanche. This assumption has been difficult to validate in part because we have lacked the tools for measuring the mechanical properties of layers both quickly and quantitatively.

Recently, micropenetrometers have come into use (c.f., Pielmeier, 1998, 2003). These portable devices can measure the penetration resistance of multiple layers in a just a few minutes. Unlike slide hammer penetrometers (e.g., Rammesonde), they have high resolution (<0.1 mm) and are sensitive to small changes in snow texture. When used repeatedly over an area, they can delineate the spatial variability of the mechanical properties of a layer (Kronholm and others, in press; McCollister and others., in press). To date, spatial studies of this nature have been done in mountain areas because that is where avalanches occur, but perhaps there are better locations for understanding the fundamental nature of snow variability. It is well known that mountain topography, with its interaction with wind and storm tracks, produces large lateral gradients in snow layers (Seligman, 1936; Mellor, 1965; Kind, 1981; McClung and Schaerer, 1993). These extreme variations can mask general trends and make it difficult to identify the sources controlling the spatial variability, which is what we really would like to know. An alternate approach is to look at the mechanical variability in flat locations where topography is not the prime source of snow heterogeneity. That was the approach used in the study reported here, where we have compared the local (≈ 1 m) and the regional (≈ 100 km) variability of the mechanical properties of snow layers in northern Alaska. Benson and Sturm (1993) and Li and Sturm (2003) have reported on the general nature of this snow cover.

Location and Methods

In March and April, 2002, we conducted a 1000-km over-snow traverse between Nome and Barrow, Alaska. The main purpose of the traverse was to determine the depth and characteristics of the snow cover across the region to assess the impact of the snow on climate and soil thermal regime. At 83 stations along the traverse route, extensive

measurements of the snow distribution and properties were made. These included a series of measurements of mechanical properties using a micropenetrometer.

Here we focus on measurements made at 10 adjacent stations spanning 325 km in the middle of the traverse route (Fig. 1). At these stations, the stratigraphy (as revealed in detailed snow pits) indicated a ubiquitous hard wind slab overlying multiple layers of depth hoar, some of which had originally been deposited by the wind. The slab and depth hoar layers could be cross-correlated with confidence across the entire 325 km, despite some regional gradations in layer properties. At each of the 10 stations, five closely spaced resistance profiles spanning 0.8 m were recorded using the Snow MicroPen (hereafter the “SMP”) mounted on a special sled (Fig. 2). The sled was also the packing case for the instrument, protecting it during travel. The SMP, its theory of operation, and application in field studies has been described by Johnson and Schneebeli (1998; 1999), Schneebeli and Johnson (1998), Schneebeli and others (1999), and Kronholm and others (in press).

Immediately adjacent to where the SMP profiles were measured, detailed measurements of stratigraphy, density, and grain size were made in a 1-m wide snow pit. These were augmented by assignment of standard hand hardness values (fist-finger-pencil-knife; Colbeck and others (1992)) for each layer. Indentation hardness was also measured using a spring device that was pushed into the side of a snow layer until failure. This spring-loaded device had various size plates that screwed onto the end of the spring shaft, giving it a large range of resistances (1 to 10,000 N). To round out the measurements, snow depth was measured at a 0.5-m spacing along a 100-m line radiating from the pit, with data from five ancillary snow pits along this line to indicate the spatial variability of the stratigraphy and snow hardness.

SMP Data Analysis

Each SMP profile consisted of a set of resistance force values (F) vs. depth (z) with z adjusted so that $z = 0$ indicated the top of the snow. The cold, dry weather in which the SMP was used resulted in a static build-up on a capacitor in the device. This superimposed a linear ramp on the force signal. It has been removed by fitting a line to the signal using a least-squares regression technique, then subtracting the linear fit from the signal. In cases where the snow was very hard (resistance values in excess of 10N), a high frequency, low amplitude chatter was present that has been removed using a binomial smoothing filter.

The filtered and de-ramped force vs. depth ($F(z)$) values (Fig 3a) were then decomposed into a local (smoothed) force ($F_T(z)$; Fig. 3a) and a residual about this smoothed force ($F_d(z)$; Fig. 3b). This was done by fitting a smoothing spline to the $F(z)$ data while visually inspecting the results to ensure that the spline captured the local trend (over distances of about 1 mm), but not the saw-tooth variations about that trend. Subtracting $F_T(z)$ from $F(z)$ produced a saw-toothed residual record where each rupture of a structural element (i.e., the breaking of a grain bond) was represented by a rapid drop in force (Fig. 3b). Using a peak-picking routine, we then produced from the residual record a discrete set of peak and valley points (*black diamonds*, Fig. 3b) that could be interpreted as a continuous record of structure element rupturing as the SMP pushed through the snow. In a typical record spanning 40 cm of snow depth, about 150,000 points in the raw data with resistance force values varying between 0 and 16N would delineate about 8,000 ruptures. Individual ruptures would drop the resistance about 0.05 to 0.1N each time as a bond/grain structure failed. Dividing 16N by 0.1N, it can be seen that on the order of 160 structural elements were providing the back resistance to the moving SMP at any given time.

By making the assumption that two structural elements never ruptured simultaneously, the estimate of the number of structural elements engaged with the SMP at any given time could be computed. This estimate is a measure of the grain and bond density per unit volume of snow. Discussions of the statistics and physics of grain bond formation can be found in Hobbs and Mason (1964), Hobbs and Radke (1967), Keeler (1969), and Gubler (1982). It was also necessary to assume that the resistance from each structural element increased linearly from zero to a maximum at rupture. At the moment that the i^{th} rupture occurred in the snow, N -structural elements would have been in contact and resisting the downward motion of the SMP. Some of these grains would just have come into contact and would be providing relatively little back resistance, while others like the i^{th} grain would have been in contact for some time, have been deflected to, or close to, their maximum displacement, and would therefore be providing nearly the maximum back resistance.

Expanding on the theoretical development of Johnson and Schneebeli (1999), we can write the total resistance force against the SMP as the sum of the resistances of each structural element in contact with the SMP:

$$F_T(z) = \bar{F}_R \left\{ 1 + \left(1 - \frac{\Delta d_1}{D_{RN}}\right) + \left(1 - \frac{\Delta d_2}{D_{RN}}\right) + \dots + \left(1 - \frac{\Delta d_N}{D_{RN}}\right) \right\} \quad [1]$$

where the \overline{F}_R indicates the mean local structural element rupture force, D_{RH} is the deflection distance to rupture of a structural element (assumed locally to be constant), and Δd_k indicates the distance the SMP travels from the i^{th} rupture before the k^{th} rupture occurs ($k=1, 2, 3 \dots$ to N). Each term in brackets on the right-hand-side of Equation [1] represents the fraction of its total rupture strength contributed by the k^{th} element. These terms decrease from 1 to 0 moving from left to right.

Computationally, we initially do not know N or D_{RN} , so we do not know how many terms to include in Equation [1]. However, we can assume a large value of D_{RN} , make a rough estimate of N , then re-compute Equation [1] using this reduced number of terms. By iterating through this process until we have reproduced $F_T(z)$ using a minimum value of D_{RN} and N , we are able to solve for N and D_{RN} . We can then compute the characteristic structural length, L :

$$L_i = \sqrt[3]{\frac{6r_p^2 \Delta z}{N}} \quad [2]$$

where r_p is the radius of the SMP tip, Δz is distance from the SMP tip to the last (most distant) structural element engaged by the SMP, and N is the number of elements in the cylindrical volume defined by r_p and Δz . We set the cylindrical volume equal to the volume of a collection of spheres of radius $L_i/2$.

Results

SMP results from two stations are shown in **Figures 4a and 4b**. At Station SA1T, the slab at the top of the snow pack had a relatively constant thickness (160 mm), resistance strength (4N), and internal stratigraphy across the 0.8 m spanned by the measurements. At Station SA6T, 89 km farther east, the slab was more variable in both strength and thickness, with a peak resistance force that ranged from 3 to 16N in less than a meter. The underlying depth hoar was also more variable at the latter station, in some locations exhibiting resistance forces as high as 2N, while at others having less than 0.5N for the same layer. As a consequence of these differences, cross-correlation of layers between adjacent profiles was easier at SA1T than at SA6T.

Using Equations [1] and [2] we have computed values of:

<i>Number of structural elements engaged with the SMP:</i>	N
<i>Rupture force of the i^{th} structural element:</i>	F_{Ri}
<i>Characteristic length of the i^{th} structural elements:</i>	L_i

for each rupture (*i*) (or alternately, for each SMP record as a function of depth (*z*)) at SA1T and SA6T. The forces required to rupture bonds were two to three times higher at SA6T than SA1T (Figs. 5a and 5b), accounting for the higher overall strength of the top slab. At any one time, slightly more grains were involved with the SMP, and the microstructural length was commensurately larger at SA6T. These differences suggest that the slabs at the two locations originated in a similar fashion (wind transport), that they had similar grain sizes due to wind pulverization, but that the bonds at SA6T were thicker and stronger, probably because the sintering processes were more intense at this station. In contrast, the underlying depth hoar had slightly stronger bonds at SA1T than SA6T, with fewer structural elements engaged at any one time with the SMP. The depth hoar structural elements were also 50% smaller. Snow pit measurements from the two sites (Table 2) are reasonably consistent with these differences indicated by the SMP.

All 50 SMP profiles from the 10 stations listed in Table 1 are shown in Figure 6. In order to emphasize the shape and pattern of the profiles, we have shifted each profile so that the snow surface is at 500 mm. This has had the effect of aligning all of the surface wind slabs. We have purposely not shown the local groupings (groups of 5 profiles per station) to further emphasize the pattern. Four types of patterns emerge:

Type 1: thick slabs of uniform strength,

Type 2: thick slabs of varying strength with depth,

Type 3: thin, hard slabs,

Type 4: absent slabs.

In some cases (i.e., second panel down), Type 2 slabs are present both locally ($\mathcal{O}\approx 1$ m) and regionally ($\mathcal{O}\approx 10$ to 100 km), with the boundary between the two scales hard to determine. In fact, slab thickness *and* internal stratigraphy are surprisingly persistent between these stations which are more than 10 km apart. In other cases Type 1 slabs make up one local group, but Type 3 make up the adjacent group, making it easy to distinguish between the two. While this suggests that the local mechanical variability is more similar than the regional variability, we note that embedded in each of these local groups is at least one profile of a distinctly different type. These produce local transitions that are as abrupt as any of the regional transitions. Finally, we note that where Type 3 patterns were present, Type 4 patterns were also common.

The foregoing measurements were all made in dry snow where wind-drifting was the primary agent producing mechanical heterogeneity. A set of measurements spanning about 10 meters width taken in the subarctic snow cover near Fairbanks that had been subjected to a thaw suggests a similar spatial scale of the local heterogeneity. Figure 7 shows a contour

map of resistance strength across the 10-m profile. The melt crust varied from 0 to 30 mm in thickness, and its resistance strength varied from near 0 (where the crust was absent) to 70N.

Discussion

We attribute the large local variance in the mechanical strength of the layers to the wind. Local wind eddies and gusts, interacting with surface roughness (keep in mind sample locations were flat), produced undulating layers comprising ripple marks, small dunes, and barchans (c.f. Douami, 1967) that varied on a scale length that ranged from less than a meter to about 100 meters. Hard and soft areas corresponding to stoss and lee slopes were present. For layers associated with melting and water percolation, the scale of variance of the mechanical properties was equally small. In this study, only depth hoar layers were somewhat uniform locally, and even for these, the regional variation in strength was not much greater than local variation. Our data largely agree with previous studies that looked at the scaling of mechanical properties (Conway and Abrahamson, 1984; Birkeland and others, 1995; Takeuchi and others, 1998; Pielmeier, 1998, 2003; Kronholm and others, in press). The data suggest that even in the absence of significant topography, a high degree of natural local variance in mechanical strength is likely. The findings of this study complement a recent study by Sturm and Benson (in press) which examined the continuity of snow layers in both seasonal and perennial snow covers. They found that variance, or heterogeneity in properties, increased up to order of 100-m, then barely increased any more as the lateral scale was increased to several hundred kilometers.

For wind slabs in particular, we found that large local variances in strength could be expected if the slab was thin (Fig. 6). When this was the case, the “normal” pinching and swelling of the layer resulted in locations where the layer was entirely absent, and a commensurately large lateral variation in mechanical strength. Conversely, where a storm deposited a heavy load of snow in the form of a wind slab, the lateral continuity, even in some of the finer features of the strength, persisted over more than 10 km. From these results, we speculate that maximum local variation in mechanical properties will be found on thinner rather than thicker layers. Unfortunately from the standpoint of avalanche prediction, weak layers tend to be thin, not thick.

Conclusions

Using micropenetrometer data collected on a traverse in NW Alaska, as well as ancillary data collected near Fairbanks, we have investigated the scale at which layer mechanical properties vary. In addition to the bulk snow layer properties revealed by resistance to penetration and standard snow pit measures (like density), we have used a

micro-mechanical theory to extract grain-scale data from the micropenetrometer measurements. In this theory, the high-frequency residual saw-tooth response of the micro-pen is converted into grain size, pore size, and bond strength as a function of depth. The theory is still preliminary, but appears to produce reasonable and interpretable grain-scale values that are similar to those determined in a more traditional manner.

The results show that layer mechanical properties vary over small distances (less than a meter), particularly when the layers in question are thin. Conversely, for thick wind slabs that are the result of significant storm deposition, the lateral continuity of the layer strength over as much as 10 km, is remarkably good. This raises some troubling issues for the use of the micropen in avalanche studies. Even larger variations than the ones detailed here are likely to be found in mountain locations where avalanches are prevalent, produced by the interaction of weather and steep slopes. These will tend to mask the underlying causes of the variability and make causal analysis difficult. While seemingly indirect, perhaps the best way toward a comprehensive understanding of layer mechanical variability is to conduct experiments in locations where this variability is limited, and the number of the controls over the spatial variability accordingly reduced. One way to do this is to avoid complex and steep topography and conduct studies where it is flat.

The implications of the findings of this study with respect to avalanches are a) that very large ranges in layer strength and properties are to be expected over short distances, particularly in mountain settings, but b) it may be possible to measure the full local range of properties across relatively short (10-m) transects, thereby generating statistical sets of for snow strength relatively easily and in locations that have lower avalanche risk. The challenge now is to figure ways to use these type of data to constrain forecasts that include snow strength or other mechanical attributes of the snow.

Acknowledgements

We thank Eric Pyne, Ken Tape, April Cheuvront, and Glen Liston for assistance in the field. Martin Schneebeli, Kalle Kronholm, and Karl Birkeland provided encouragement and technical support. The work was support by the U.S. Army AT-24 Program, and by the National Science Foundation Office of Polar Programs-Arctic System Science Program.

References

- Benson, C. S., and M. Sturm, 1993: Structure and wind transport of seasonal snow on the Arctic slope of Alaska, *Annals of Glaciology*, **18**, 261-267.
- Birkeland, K. W., K. J. Hansen, and R. L. Brown. 1995. The spatial variability of snow resistance on potential avalanche slopes. *J. of Glaciol.*, *41*(137), 183-190.
- Birkeland, Karl W.; Johnson, Ron; Herzberg, Diane. 1996. The stuffblock snow stability test. *Tech. Rep. 9623-2836-MTDC*. Missoula, MT: U.S. Department of Agriculture, Forest Service, Missoula Technology and Development Center. 20 p.
- Conway, H. and J. Abrahamson. 1984. Snow stability index. *Journal of Glaciology*, *30* (106), 321-327.
- Colbeck, S. C. 1991. The layered character of snow covers. *Reviews of Geophysics* *29*: 81-96.
- Colbeck, S. C., and J. B. Jamieson. 2001. The formation of faceted layers above a crust. *Cold Regions Science and Technology* *33*: 247-252.
- Colbeck, S., E. Akitaya, R. Armstrong, H. Gubler, J. Lafeuille, K. Lied, D. McClung, and E. Morris. 1992. *The International Classification for Seasonal Snow on the Ground*. Pages 23. The International Commission on Snow and Ice of the International Association of Scientific Hydrology/International Glaciological Society/U.S. Army CRREL, Hanover, New Hampshire.
- Davis, R. E., J. B. Jamieson, J. Hughes, and C. Johnston. 1996. Observations on buried surface hoar-persistent failure planes for slab avalanches in British Columbia, Canada. *Proceedings of the International Snow Science Workshop*, Banff, BC : 81-85.
- Davis, R. E., J. B. Jamieson, and C. Johnston. 1998. Observations on buried surface hoar in British Columbia, Canada: Section analyses of layer evolution. *Proceedings of the International Snow Science Workshop*, Sun River, Oregon : 86-92.
- Doumani, G. A. 1967. Surface structures in snow. In *Physics of Snow and Ice*, Vol. 1, H. Oura, ed. *Institute of Low Temp. Sci.*, Hokkaido University, Sapporo, 1119-1136.
- Fierz, C. 1998. Field observations and modeling of weak-layer evolution. *Annals of Glaciology* *26*: 7-13.
- Föhn, P. M. B. 1987. The "Rutschblock" as a practical tool for slope stability evaluation. *Inter. Assoc. of Hydrological Sciences Publication 162* (Symposium at Davos 1986-Avalanche formation, movements and effects), 223-228.
- Gubler, H. 1977. Artificial release of avalanches by explosive, *J. Glaciol.*, *19*(81), 419-429.
- Gubler, H. and H. P. Bader. 1989. A model of initial failure in slab-avalanche release. *Ann. of Glaciol.* *13*, 90-95.
- Gubler, H. 1982. Strength of bonds between ice grains after short contact times. *J. of Glaciol.* *28* (100), 457-474.

- Hobbs, P. V. and B. J. Mason. 1964. The sintering and adhesion of ice. *Phil. Mag.* 9, 181-197.
- Hobbs, P. V. and B. J. Radke. 1967. The role of volume diffusion in the metamorphism of snow. *J. of Glaciol.* 6 (48), 879-891.
- Jamieson, J. B. and C. D. Johnston. 1993. Rutschblock precision, technique variations and limitations. *J. of Glaciol.* 39(133), 666-674.
- Johnson, J.B. and M. Schneebeli. 1998. Snow strength penetrometer. U. S. Army Corps of Engineers, U. S. Patent and Trademark Office No. 08/850,160.
- Johnson, J. B. and M. Schneebeli, 1999. Characterizing the microstructural and micromechanical properties of snow. *Cold Regions Science and Technology*, 30, 91-100.
- Keeler, C. M. 1969. The growth of bonds and the increase of mechanical strength in a dry seasonal snow-pack. *J. of Glaciol* 8 (54), 441-450.
- Kind, R. J. 1981. Snow Drifting, Chapter 8, in *Handbook of Snow*, eds. D. M. Gray and D. H. Male, Pergamon Press, Toronto, 338-359.
- Kronholm, K., M. Schneebeli, and J. Schweizer. In press. Spatial variability of micropenetration resistance in snow layers on a small slope. *Annals of Glaciology* 34.
- Li, S. and M. Sturm. 2003. Patterns of Wind-Drifted Snow on the Alaskan Arctic Slope Detected with ERS-1 Interferometric SAR. *J. of Glaciol.*
- McClung, D., and P. Schaerer. 1993. *The Avalanche Handbook*. The Mountaineers, Seattle.
- McCollister, C., K. W. Birkeland, and K. Hansen. In Press. Exploring the spatial variability of hard slab and dry loose avalanches, Jackson Hole, Wyoming, U.S.A. *Annals of Glaciol.*
- Mellor, M. 1965. Blowing Snow. CRREL *Cold Regions Science and Engineering* Part III, Section A3c. 79pp.
- Pielmeier, C. 1998. *Analysis and discrimination of snow structure and snow profiles using a high resolution penetrometer*. MSc. Thesis, Ludwig-Maximilians Universität, München, Germany.
- Pielmeier, C. 2003. *Textural and mechanical variability of mountain snowpacks*. Ph.D. Thesis, Universität Bern, Switzerland, 127 pp.
- Schneebeli, M., C. Pielmeier and J. B. Johnson, 1999. Measuring snow microstructure and hardness using a high resolution penetrometer. *Cold Regions Science and Technology*, 30, 101-114.
- Schneebeli, M. and J.B. Johnson. 1998. A constant speed penetrometer for high resolution snow stratigraphy. *Annals of Glaciol.*, 26, 107-111.
- Seligman, G. 1937. *Snow Structure and Ski Fields*, Int. Glaciol. Society, Cambridge, 553 pp.

- Smith, F. W. and R. A. Sommerfeld. 1985. The simulation of statistical failure of snow slopes. *Simulations Series*, 15(1), 29-33.
- Sturm, M. And C. S. Benson. In press. Scales of Spatial Heterogeneity for Perennial and Seasonal Snow Layers. *Annals of Glaciol.* 34.
- Takeuchi, Y., Y. Nohguchi, K. Kawashima, K. Izumi, 1998. Measurements of snow hardness distribution. *Annals of Glaciol.*, 26, 27-30.

List of Figures

Figure 1: Northwest Alaska showing the SnowSTAR 2002 traverse route.

The stars indicate the locations of stations where mechanical properties were measured using the Snow MicroPen. The total length of the traverse line was 1000-km.

Figure 2: The Snow MicroPen mounted on a 5-position sled. The computer used to operate the SMP was housed in the heated sled (background). It was pulled by a snowmobile (left rear). When not in use, the SMP was packed into the 5-position sled surrounded by the packing material.

Figure 3: a) Resistance to penetration (N) as a function of depth in the snow, with an inset showing a smoothed force curve fitted to the data using a cubic smoothing spline. b) residual force (force-smoothed force) saw-tooth record (red) and peaks and valleys (black diamonds) identified in this record using a peak-picking routine. The segment shown corresponds with the inset in Figure 3a. The data are from Station SA6T.

Figure 4: a) Five adjacent SMP profiles from Station SA1T. b) Five adjacent SMP profiles from Station SA6T, 89 km from SA1T. Dotted lines show probable layer correlations between adjacent SMP profiles.

Figure 5: a) Microstructural parameters computed for Stations SA1T and SA6T, Push 1. The heavy black lines are smoothed data (binomial filter, 200 passes); the colored lines the actual data, which fluctuate widely. Panels are, from left to right, *Force*, *Rupture Force*, *Involved Grains*, and *Microstructural Length*.

Figure 6: Layer penetration force results from all 10 stations, plotted on the same scale, but with the top of the snow set to 500 mm to emphasize the similarities in pattern. See text for the definition of the 4 types of patterns.

Figure 7: Penetration resistance from the subarctic snow pack near Fairbanks, Alaska. There had been a thaw and a melt crust had formed, along with some minor percolation columns. The remainder of the snow pack was weak depth hoar. The melt crust is delineated by the zone in excess of 5N resistance force.

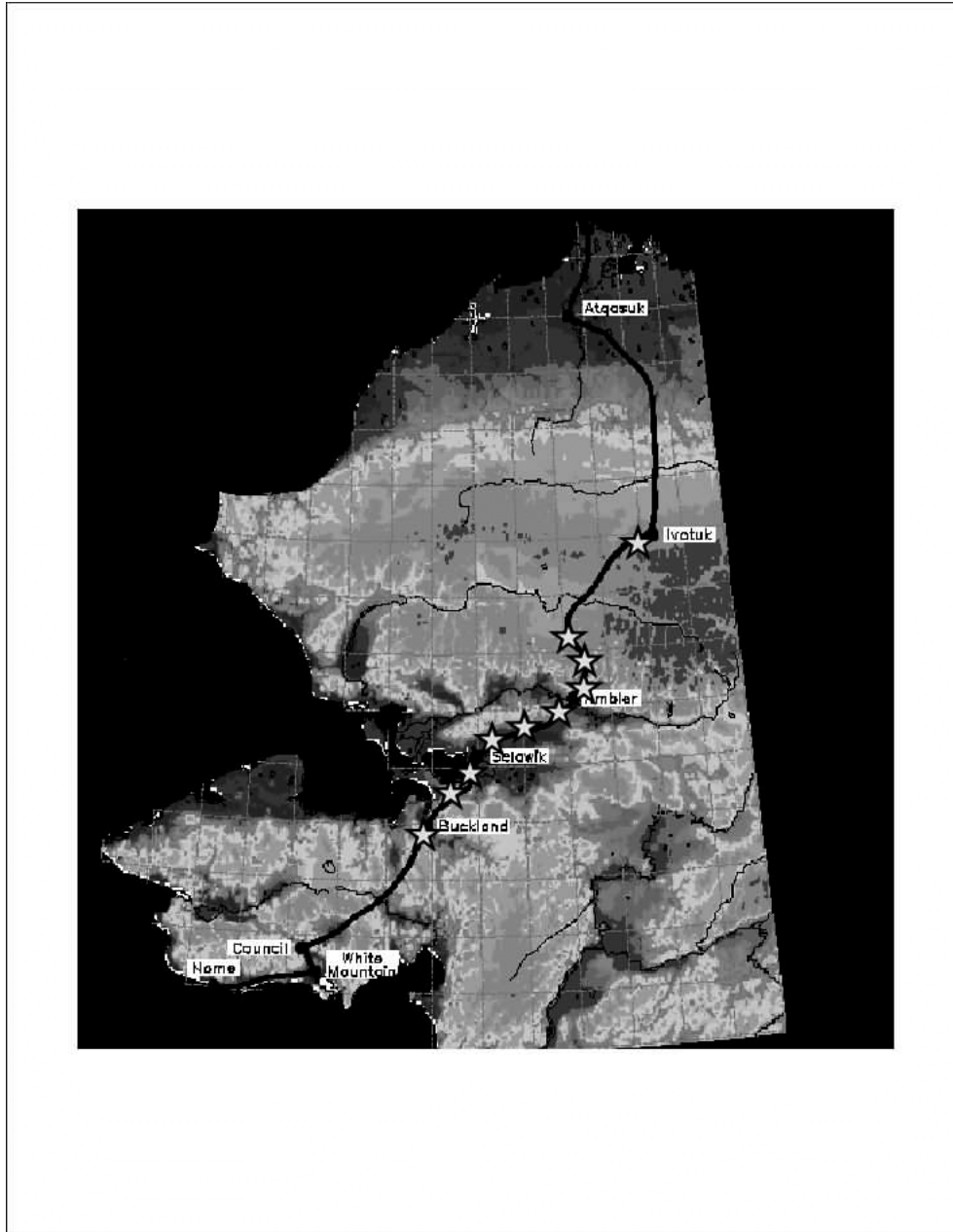


Figure 1: Northwest Alaska showing the SnowSTAR 2002 traverse route. The stars indicate the locations of stations where mechanical properties were measured using the Snow MicroPen. The total length of the traverse line was 1700-km.

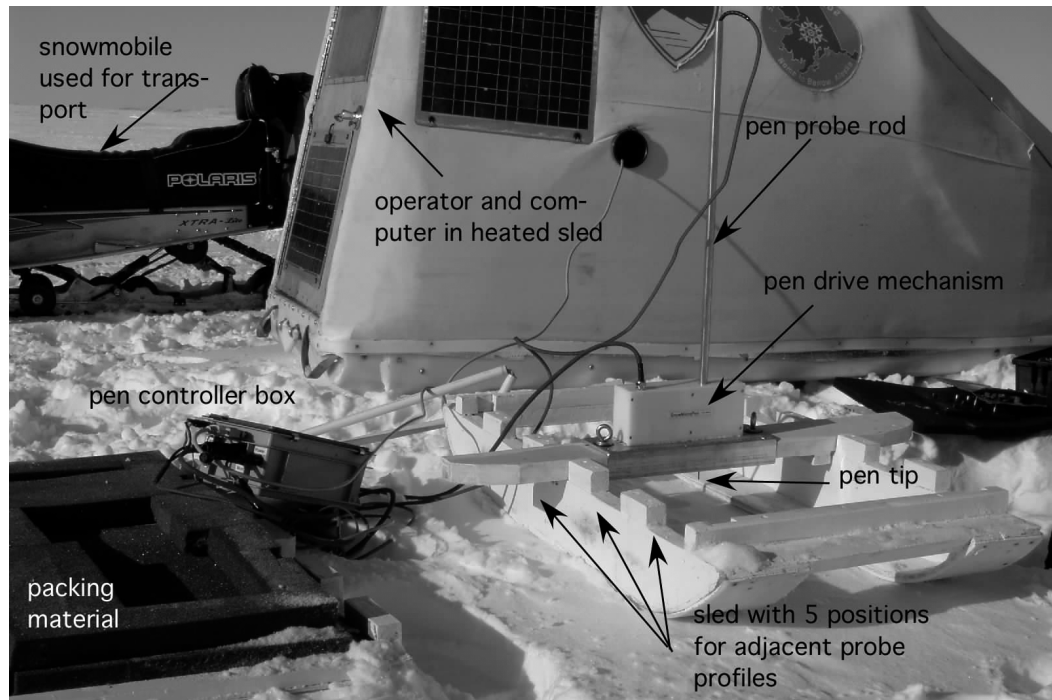


Figure 2: The Snow MicroPen mounted on a 5-position sled. The computer used to operate the SMP was housed in the heated sled (background). It was pulled by a snowmobile (left rear). When not in use, the SMP was packed into the 5-position sled surrounded by the packing material.

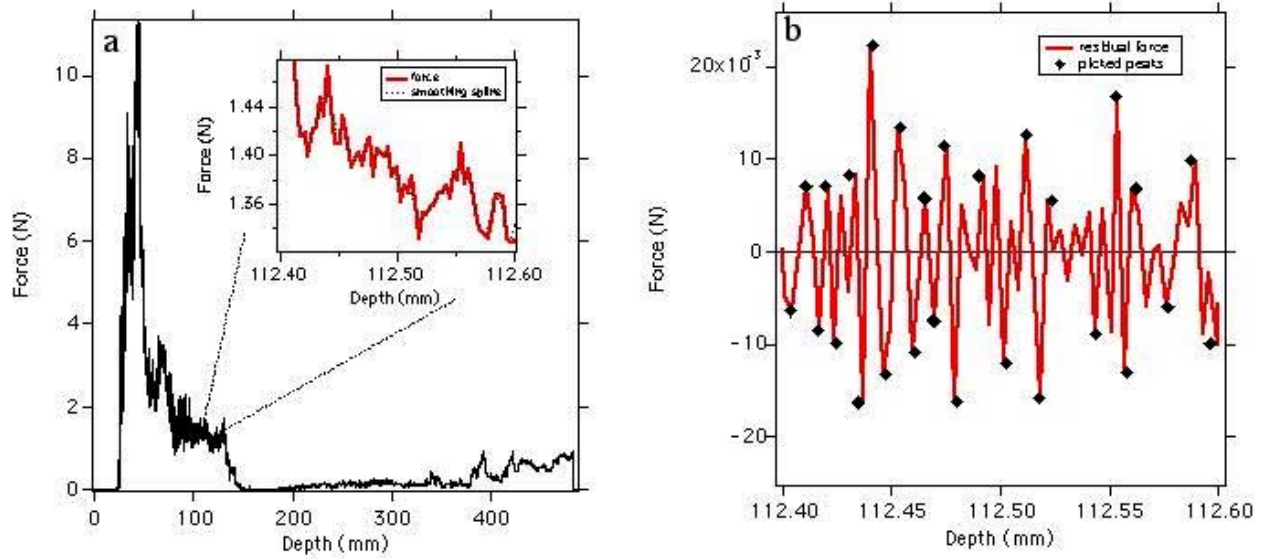


Figure 3: a) Resistance to penetration (N) as a function of depth in the snow, with an inset showing a smoothed force curve fitted to the data using a cubic smoothing spline. b: residual force (force-smoothed force) saw-tooth record (red) and peaks and valleys (black diamonds) identified in this record using a peak-picking routine. The segment shown corresponds with the inset in Figure 3a. The data are from Station SA6T.

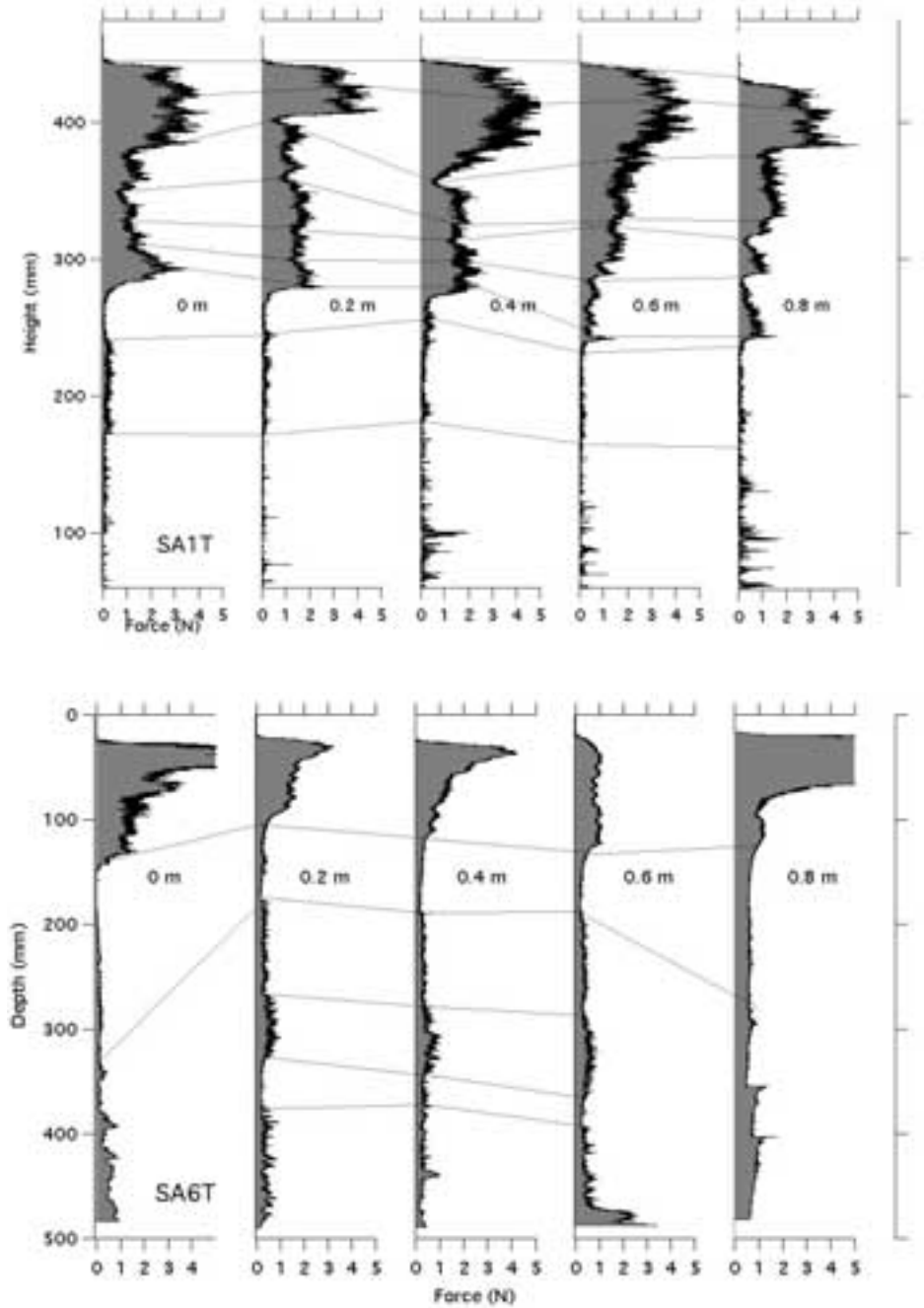


Figure 4: a) Five adjacent SMP profiles from Station SA1T. b) Five adjacent SMP profiles from Station SA6T, 89 km from SA1T. Dotted lines show probable layer correlations between adjacent SMP profiles.

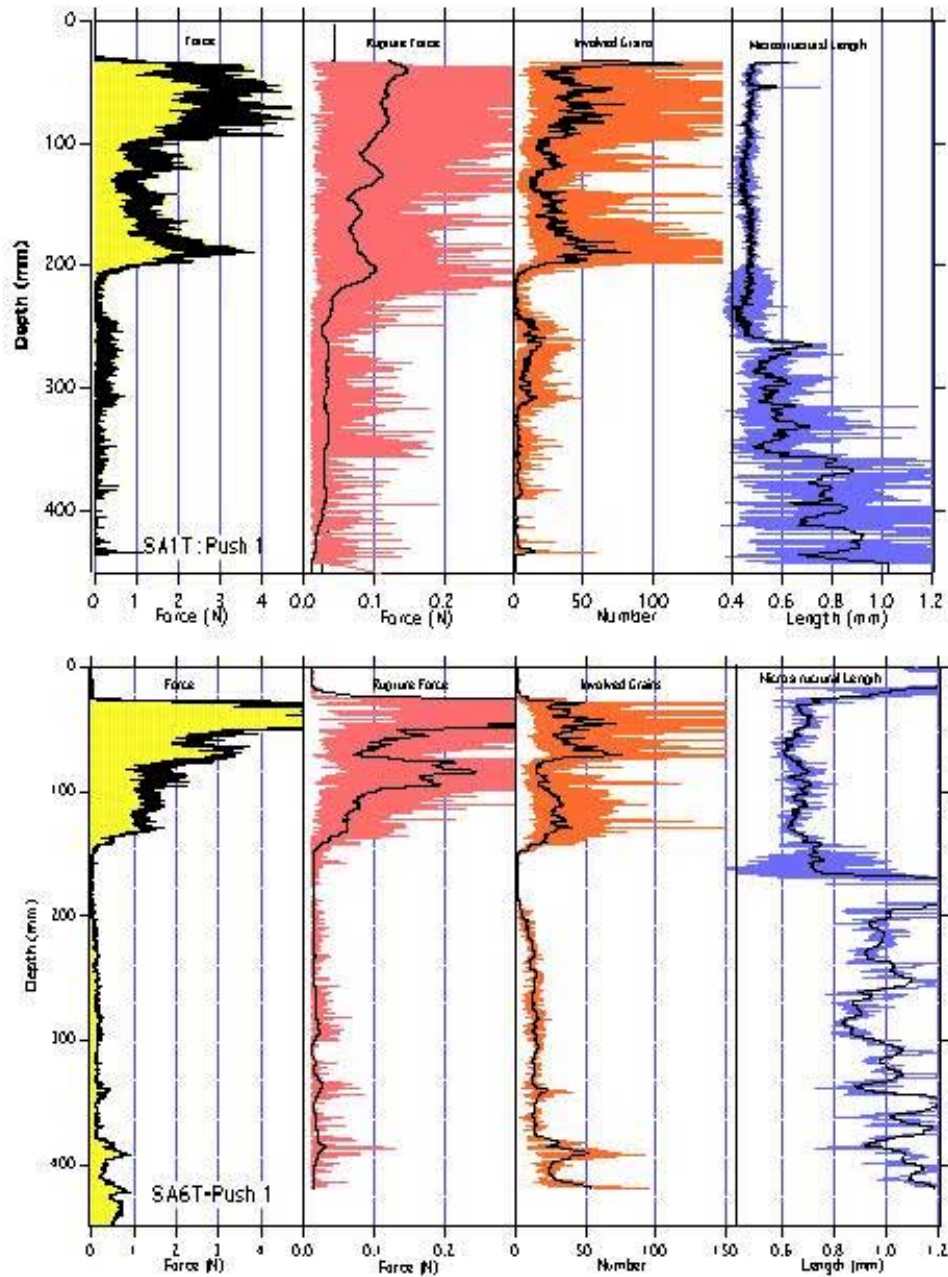


Figure 5: a) Microstructural parameters computed for Stations SA1T and SA6T, Push 1. The heavy black lines are smoothed data (binomial filter, 200 passes); the colored lines are the actual data, which fluctuate widely. The panels are, from left to right, Force, Rupture Force, Involved Grains, and Microstructural Length.

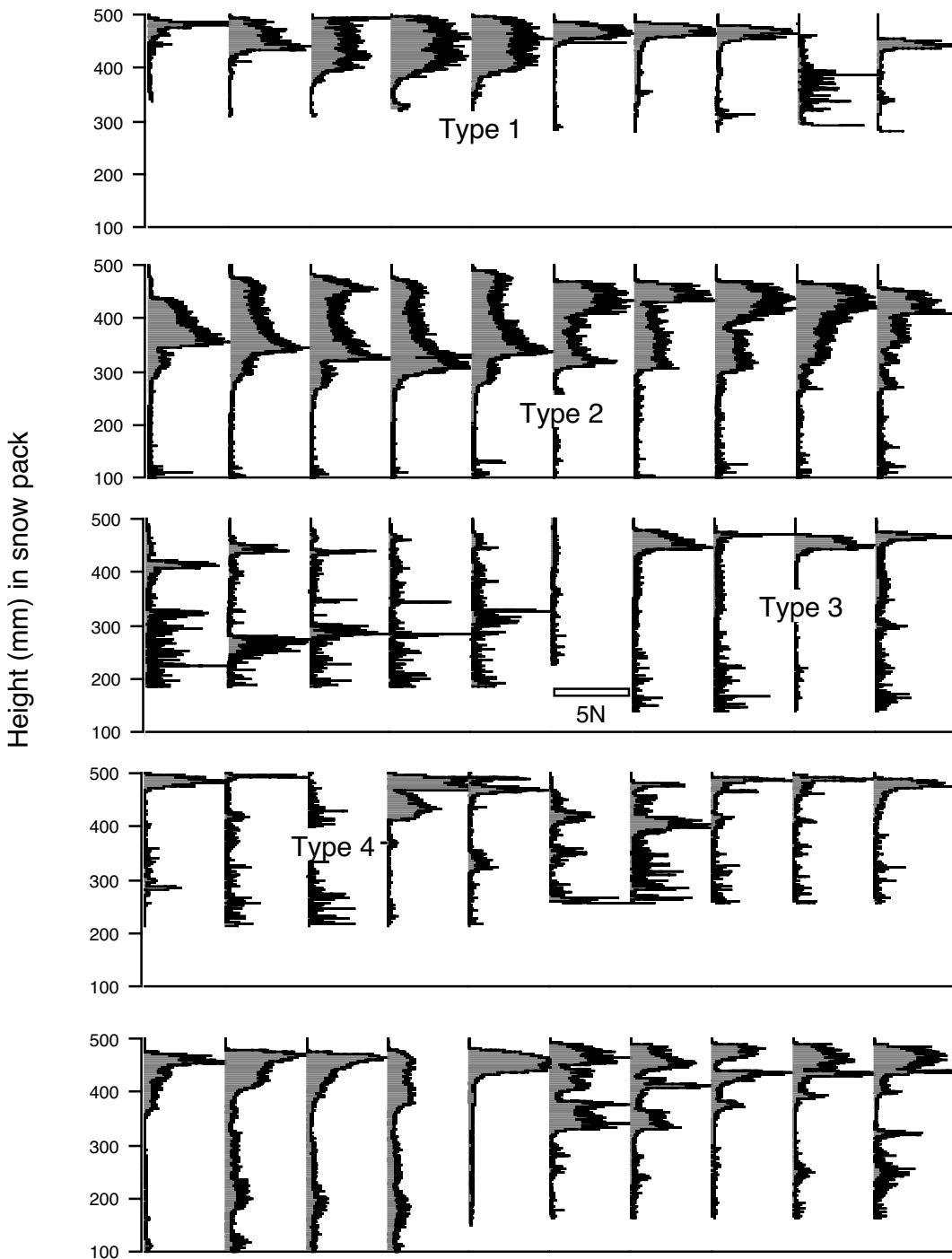


Figure 6: Layer penetration force results from all 10 stations, plotted on the same scale, but with the top of the snow set to 500 mm to emphasize the similarities in pattern. See text for the definition of the 4 types of patterns.

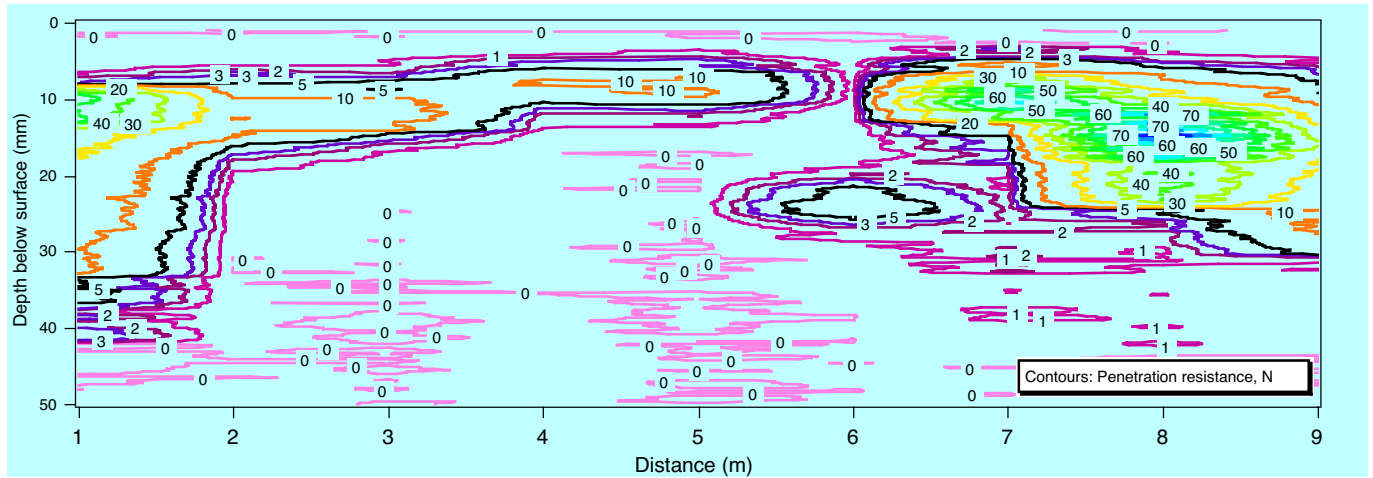


Figure 7: Penetration resistance from the subarctic snow pack near Fairbanks, Alaska. There had been a thaw in which a melt crust had formed, along with some minor percolation columns. The remainder of the snow pack was weak depth hoar. The melt crust is delineated by the zone of contours in excess of 5N resistance force.

Table 1: Station locations

Station	Latitude (dd.ddddd)	Longitude (dd.ddddd)	Distance (km)	Ave. Depth (cm)	Std. dev. (cm)
BS2t	66.2477169	-160.829132	0	20.0	10.1
BS3t	66.3339041	-160.535311	16	22.9	6.7
SA1u	66.605056	-159.02046	80	49.9	10.1
SA1t	66.625231	-159.58046	90	40.9	8.8
SA2t	66.6603881	-159.186782	108	56.8	10.9
SA3t	66.7203196	-158.808696	126	39.5	12.8
SA4t	66.7665525	-158.384058	145	42.7	10.5
SA5t	66.8727169	-158.157971	160	36.8	10.6
SA6t	67.0148402	-157.918129	179	28.9	12.9
AI9	68.1261416	-156.184848	324	43.7	9.2

Table 2: Layer characteristics at Stations SA1T and SA6T

	Thickness (cm)	Density (g/cm ³)	Hand Hardness	Indentor Force (N)	Grain Size (mm)
SA1T, top slab	18	0.39 to 0.45	pencil	5000-9000	0.2 to 1.0
SA6T, top slab	10	0.40 to 0.52	pencil to knife	7500 to 10500	0.6 to 1.3
SA1T, top hoar layer	3	0.31	3 fingers	550 to 600	1.0 to 2.0
SA6T, top hoar layer	7	0.24	3 fingers	160 to 400	1.5
SA1T, middle hoar layer	6	0.24	fist	75	1.5 to 2.0
SA6T, middle hoar layer	5	0.24	fist	120	3.0 to 4.0
SA1T, lower hoar layer	17.5	0.22	fist	80	2.0 to 8.5
SA6T, lower hoar layer	12	0.26 to 0.29	fist	400	4